



PB98-102395

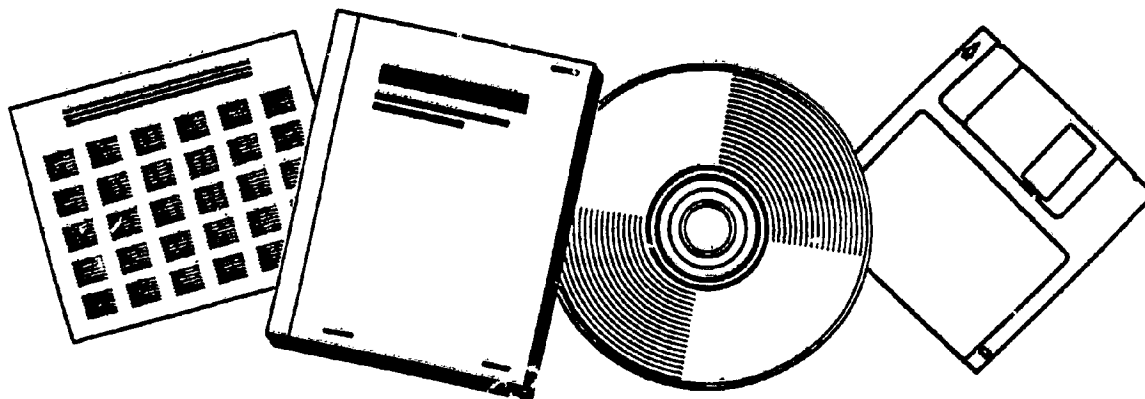
**NTIS**<sup>®</sup>  
Information is our business.

---

## **IMPULSE RESPONSE MEASUREMENTS OVER SPACE-EARTH PATHS USING THE GPS COARSE/ACQUISITION CODES**

**(U.S.) NATIONAL TELECOMMUNICATIONS AND INFORMATION  
ADMINISTRATION, BOULDER, CO**

**SEP 95**



**U.S. DEPARTMENT OF COMMERCE  
National Technical Information Service**

---



P

NTIA Report 95-324



PB96-102395

# **Impulse Response Measurements Over Space-Earth Paths Using the GPS Coarse/Acquisition Codes**

**John J. Lemmon**



***report series***

---

U.S. DEPARTMENT OF COMMERCE • National Telecommunications and Information Administration

---



# **Impulse Response Measurements Over Space-Earth Paths Using the GPS Coarse/Acquisition Codes**

**John J. Lemmon**



**U.S. DEPARTMENT OF COMMERCE  
Ronald H. Brown, Secretary**

REPRODUCED BY  
U.S. DEPARTMENT OF COMMERCE  
NATIONAL TECHNICAL  
INFORMATION SERVICE  
SPRINGFIELD, VA 22161

Larry Irving, Assistant Secretary  
for Communications and Information

September 1995



## PREFACE

Certain commercial equipment, instruments, and software are identified in this report to specify adequately the experimental procedure. In no case does such identification imply recommendation or endorsement by the National Telecommunications and Information Administration, nor does it imply that the material or equipment identified is necessarily the best available for the purpose.





## CONTENTS

PREFACE .....	iii
ABSTRACT .....	1
1. INTRODUCTION .....	1
2. DATA ACQUISITION SYSTEM .....	3
3. SIGNAL PROCESSING .....	5
4. EXAMPLES OF IMPULSE RESPONSE MEASUREMENTS .....	6
5. RECOMMENDATIONS FOR FUTURE WORK .....	13
6. CONCLUSIONS .....	15
7. ACKNOWLEDGMENTS .....	16
8. REFERENCES .....	16



## IMPULSE RESPONSE MEASUREMENTS OVER SPACE-EARTH PATHS USING THE GPS COARSE/ACQUISITION CODES

John J. Lemmon and Peter B. Papazian<sup>1</sup>

The impulse responses of radio transmission channels over space-earth paths were measured using the coarse/acquisition code signals from the Global Positioning System of satellites. The data acquisition system and signal processing techniques used to develop the impulse responses are described. Examples of impulse response measurements are presented. The results indicate that this measurement approach enables detection of multipath signals that are 20 dB or more below the power of the direct arrival. Channel characteristics that could be investigated with additional measurements and analyses are discussed.

**Key words:** impulse response function; Global Positioning System (GPS); radio transmission channel; pseudorandom noise (PN) codes

### 1. INTRODUCTION

This report discusses measurements of the impulse response of radio transmission channels over space-earth paths. The measurements were performed using signals from the Global Positioning System (GPS) of satellites. The possibility of using GPS signals to perform such measurements was initially considered in 1985, when the Institute for Telecommunication Sciences (ITS) was asked to perform a feasibility study in support of the NASA Propagation Program. The study concluded that the structure of the GPS signals, consisting of L-band carriers that are biphase modulated with pseudorandom noise (PN) codes, would enable impulse response measurements to be made by correlating a received signal with a locally generated replica of the transmitted signal [1]. Analyses of the signal-to-noise (S/N) ratio indicated that adequate S/N ratios could be achieved to characterize the multipath, and it was recommended that a measurement campaign be conducted.

Two different kinds of PN codes are used in the GPS signals: the coarse/acquisition (C/A) codes and the precision (P) codes. The C/A codes are Gold codes of length 1023 with a chipping rate of 1.023 MHz; thus, each code word has a duration of exactly 1 ms. The P codes are extremely long codes (approximately 37 weeks) that are reset once per week and have a chipping rate of 10.23 MHz. The resolution (in time delay) of the measured impulse response is approximately one code bit duration, resulting in measurement resolutions of approximately 100 ns and 1  $\mu$ s for the P codes and the C/A codes, respectively.

---

<sup>1</sup>The authors are with the Institute for Telecommunication Sciences, National Telecommunications and Information Administration, U.S. Department of Commerce, Boulder, CO 80303-3328.

A proposal was made to perform impulse response measurements using the P codes rather than the C/A codes to obtain greater measurement resolution. Accordingly, upon receipt of NASA funding, ITS attempted to contract the development of an appropriately modified P-code receiver, as described in [2]. The proposed system was a dual-channel P-code receiver, in which the first channel would acquire and lock on to the P code. The current P-code epoch time and Doppler shift would be passed on to the second channel, in which the received signal would be correlated with a delayed, locally generated P code, enabling the development of the channel impulse response as a function of relative time delay. Unfortunately, insufficient funds precluded the development of the system, and this approach was abandoned.

An alternate approach was then proposed [3], whereby a "codeless" P-code receiver would be developed at the University of Colorado, Boulder, CO. Using a codeless approach, a single-channel receiver would be used to perform a correlation between signals received by two different antennas: a high-gain reference antenna that would not receive multipath signals and a low-gain "antenna under test" that would receive multipath signals, if any were present. Thus, the PN code received by the reference antenna would be used in place of a locally generated code in the correlation processing. An advantage of the codeless approach is that time delay and Doppler effects on the signals received by the two antennas are identical, obviating a need to know the current P-code epoch and Doppler shift; a disadvantage is the need for a high-gain antenna with the capability to track GPS satellites.

The complexity of the codeless approach and funding difficulties impeded the system development, and this approach, like the dual-channel approach discussed above, was abandoned. As an alternative to these rather complex P-code approaches, ITS investigated the feasibility of performing multipath measurements using the C/A codes. The idea was to use existing hardware to record GPS signals and perform the correlation processing in software. Because the C/A codes are known codes of 1-ms duration, they can be generated and correlated with received signals in software, so that a high-gain reference antenna and most of the hardware required in a modified GPS P-code receiver are no longer necessary. This approach therefore results in a vast simplification in hardware.

The disadvantage of using the C/A codes is the decreased resolution in time delay relative to the P codes. A resolution of  $1\ \mu\text{s}$  corresponds to a path difference of approximately 300 m; multipath may be present in some environments in which the path differences between the multipath and direct arrivals are much less than 300 m. On the other hand, impulse response data developed with the C/A codes can adequately characterize transmission channels whose bandwidths do not exceed those of the C/A-code signals (approximately 2 MHz). Thus, this data would be relevant to numerous applications of satellite communications and navigation.

Uncertainties in S/N ratios and the noise figures of the receiver and recording systems, as well as variables in the processing, made it difficult to assess the viability of this approach a priori. For example, the processing gain is a function of the integration time in the correlation processing; the integration time is in turn limited by the amount of memory in the recording system and the time scale over which the transmission channel is reasonably stationary. The objective of this work was

to investigate whether this approach can generate useful results and to determine the values of S/N that can be achieved using various processing techniques.

Section 2 describes the hardware that was used to collect the raw data. The data processing that was performed in software is described in Section 3. In Section 4, example impulse responses developed with this method are presented and discussed. Additional processing that could be performed and improvements to the measurement system that could be made are described in Section 5. Concluding remarks and recommendations for additional measurements and processing are made in Section 6.

## 2. DATA ACQUISITION SYSTEM

Figure 1 shows a block diagram of the data acquisition system. The GPS signals have right-hand circular polarization at an L-band frequency of 1575.42 MHz in the absence of Doppler effects (spacecraft motion can generate several kHz of Doppler shift). The signals are received by a right-hand circular MicroPulse GPS antenna mounted on the roof of the Boulder Laboratories, Boulder, CO. The antenna is low-gain (between +4.5 dBiC and -4.5 dBiC, depending on elevation angle) and therefore does not discriminate severely against multipath. The RF signals received by the antenna are preamplified and passed through 100 feet of RG 58 cable from the roof to the laboratory, where they are further amplified and downconverted to IF by an HP 8563A spectrum analyzer.

The second IF from the analyzer is tuned to 301.027 MHz and is mixed with the 300-MHz calibration signal after it is padded for signal conditioning, amplified, and low-pass filtered for harmonic suppression. The resulting signal spectrum is centered at 1.027 MHz (in the absence of Doppler effects). This frequency was chosen because the bandwidth (defined as the width of the central spectral lobe) of the C/A-code signals is twice the chipping rate of 1.023 MHz. Thus, the signal spectrum has been translated to as low a frequency as possible (to minimize the Nyquist requirement) without folding from negative frequencies, after allowing for as much as 4 kHz of Doppler shift. The signal is low-pass filtered for harmonic suppression and anti-aliasing, amplified, and sampled by a Lecroy 9450A digital oscilloscope. The scope is clocked and triggered by an HP 8640B signal generator.

Each sample is an eight-bit integer, and the memory in the scope allows a data file comprising 50,000 samples to be collected. The sample rate is 8.192 MHz, and was determined as follows. The highest frequency in the signal spectrum (allowing for 4 kHz of Doppler shift) is 2.054 MHz. The Nyquist rate for the channel is therefore 4.108 MHz. The digital signal processing (discussed in Section 3 below) uses Fast Fourier Transform (FFT) algorithms, which require that the number of samples in each record be equal to a power of two. Each record corresponds to a single C/A-code word, which has a duration of 1 ms. Thus, the smallest power of two, which when divided by 1 ms is greater than 4.108 MHz, is 8192. This corresponds to a sample rate of 8.192 MHz. The IF and sample rate are precisely maintained by phase locking the spectrum analyzer and signal generator to a stable 10 MHz Rubidium frequency reference. The spectrum analyzer and scope are controlled by a personal computer, which is used to store and process the data.

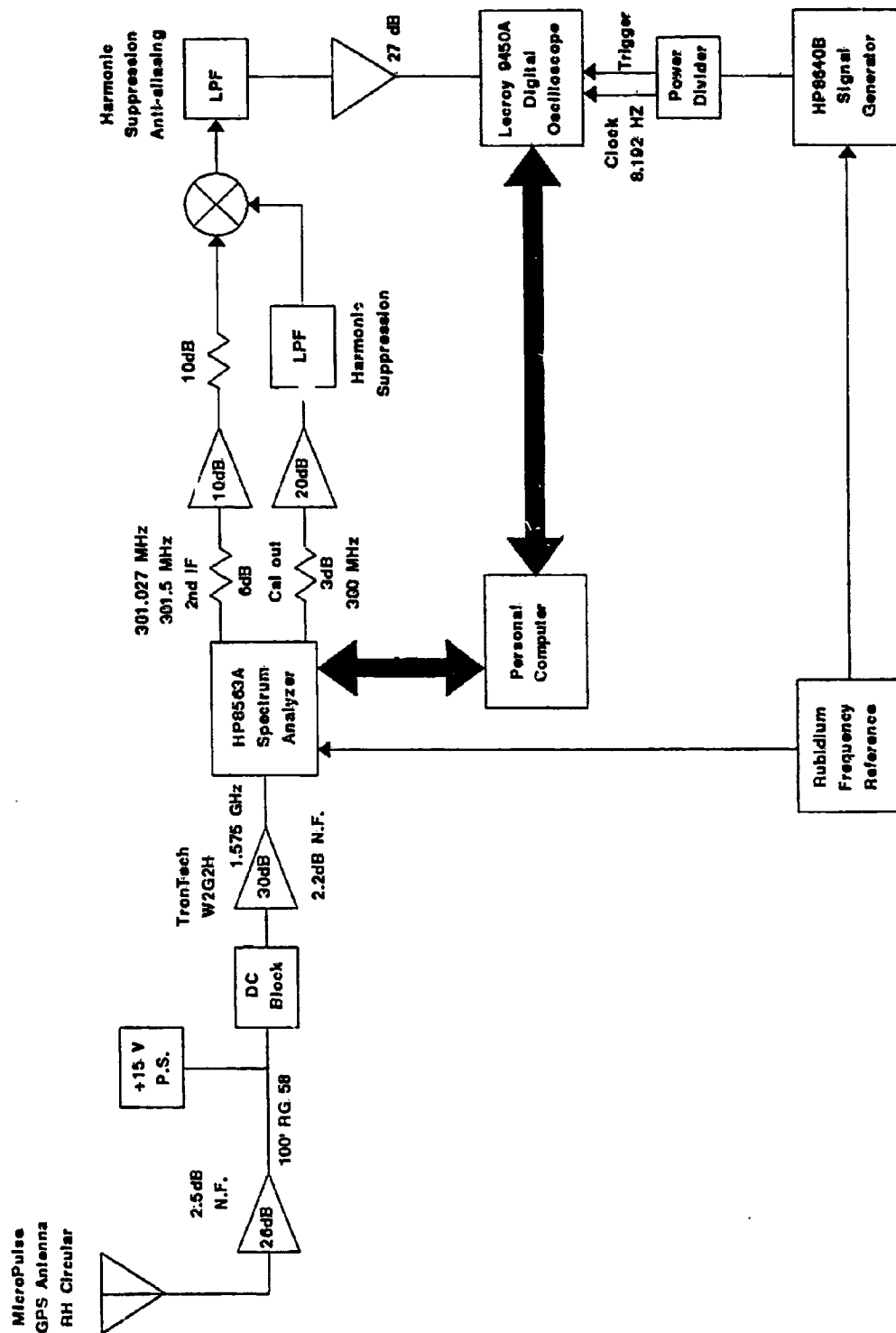


Figure 1. Data acquisition system.

### 3. SIGNAL PROCESSING

The complex, equivalent low-pass impulse response of the transmission channel was developed using the well-known technique of correlating the received signal with a locally generated replica of the transmitted signal. The correlation processing was done in the frequency domain; that is, rather than computing the cross-correlation function of the transmitted and received signals, the cross-spectral density (product of the Fourier transforms) of the signals was computed, and the result was inverse Fourier transformed back into the time domain.

To make this precise, let  $f(t)$  denote the received signal at the center frequency  $(\omega_{IF} + \omega_{DS})$ , where  $\omega_{IF}$  corresponds to the 1.027-MHz IF and  $\omega_{DS}$  is the Doppler shift. The received signal is to be correlated with a replica of the transmitted signal  $pn(t)$ , which is a pseudonoise Gold code with a binary value of  $\pm 1$ . Before computing the cross-correlation, the received and transmitted signals must be converted to the same center frequency, or the relative (time-dependent) phase between the signals will cause the cross-correlation to vanish. (Equivalently, in the frequency domain, the spectra of the signals must be centered at the same frequency or the lack of spectral overlap will cause the product of the spectra to vanish.) Because  $pn(t)$  is a baseband signal (zero center frequency), it should be correlated with the quantity

$$e^{-j(\omega_{IF} + \omega_{DS})t} f(t), \quad (1)$$

which is the received signal at baseband. The impulse response was computed as the inverse discrete Fourier transform of the cross-spectral density of the transmitted and received signals at baseband. Thus, in terms of  $f(t)$  and  $pn(t)$ , the impulse response at time  $t_0$  is

$$\int_{-\pi R_s}^{+\pi R_s} e^{+j\omega\tau} \left\{ \left[ \int_{t_0}^{t_0+T_0} pn(t) e^{-j\omega t} dt \right]^* \int_{t_0}^{t_0+T_0} f(t) e^{-j(\omega_{IF} + \omega_{DS} + \omega)t} dt \right\} d\omega, \quad (2)$$

where  $\tau$  denotes time delay,  $R_s$  is the sample rate (8.192 MHz), and  $T_0$  is the period of a code word (1 ms). The transforms are computed using FFT algorithms with time blocks equal to  $T_0$ .

The value of  $\omega_{DS}$  could, in principle, have been determined from the ephemeris data of the various satellites. However, to eliminate errors due to uncertainties in the ephemerides,  $\omega_{DS}$  was determined by computing the impulse response for all values of  $\omega_{DS}$  between +4 kHz and -4 kHz in steps of 15 Hz and using the value of  $\omega_{DS}$  for which the peak of the power delay profile (absolute square of the complex impulse response) is a maximum.

#### 4. EXAMPLES OF IMPULSE RESPONSE MEASUREMENTS

The equipment described in Section 2 was used to collect data at approximately 10:00 a.m. local time (17:00 UTC) on March 24, 1994. Two data files of 50,000 samples each were recorded at a sample rate of 8.192 MHz. The first data file was recorded with an IF of 1.027 MHz, as described in Section 2. The second data file was recorded with an IF of 1.5 MHz to investigate the effect (if any) of the IF on the impulse response measurement (the Nyquist requirement for the 1.5 MHz IF is well within the 8.192 MHz sample rate).

The GPS satellite schedule for the date and location that the data were collected was generated using public domain software (the InstantTrack program, written by Franklin Antonio), and is shown in Figure 2. Local time is indicated across the top of the diagram, and satellite numbers are listed in the vertical column at the left. The schedule indicates that as many as nine satellites may have been in view when the data were collected.

```

Day: 03/24/94
Station: BOULDER LABS

                                Hour - MST
-----0  1  2  3  4  5  6  7  8  9 10 11 12 13 14 15 16 17 18 19 20 21 22 23
BI-09 -----*****-----
BI-10 -----*****-----
BI-11 *****-----*****
BII-1 -----*****-----
BII-2 -----*****-----
BII-3 *****-----*****
BII-4 -----*****-----
BII-5 *****-----*****
BII-6 -----*****-----
BII-7 *****-----*****
BII-8 *****-----*****
BII-9 -----*****-----
BIIA-10*****-----*****
BIIA-11-----*****-----
BIIA-12-----*****-----
BIIA-13*****-----*****
BIIA-14*****-----*****
BIIA-15-----*****-----
BIIA-16-----*****-----
BIIA-17-----*****-----
BIIA-18*****-----*****
BIIA-19-----*****-----
BIIA-20-----*****-----
BIIA-21*****-----*****
BIIA-22-----*****-----
BIIA-23-----*****-----

```

Figure 2. GPS satellite schedule for Boulder, CO on March 24, 1994. The asterisks correspond to times when the satellites were above 0° elevation angle.



The data were processed using the technique discussed in Section 3. The C/A codes for the nine satellites were generated in accordance with [4]. Peaks in the cross correlation functions stand out clearly above the noise floor in five of the nine cases. The failure to detect peaks in the other four cases was presumably caused by obstructions due to low elevation angles. This was corroborated by generating the approximate azimuth and elevation angles for the nine satellites, and for the time, date, and location that the data were collected, using the aforementioned public domain software. The results are shown in Table 1. Correlation peaks were detected for those satellites at elevation angles greater than or equal to 20°, and were not detected for those satellites at elevation angles less than or equal to 15°.

Table 1. GPS Satellite Positions as Seen from Boulder, CO at 17:00 UTC on March 24, 1994

Satellite	Azimuth	Elevation	Correlation Peak Detected?
BI-11	45°	7°	No
BII-1	198°	40°	Yes
BII-4	263°	20°	Yes
BII-6	310°	45°	Yes
BIIA-13	127°	15°	No
BIIA-15	260°	0°	No
BIIA-17	342°	79°	Yes
BIIA-18	71°	61°	Yes
BIIA-19	158°	2°	No

At the 8.192 MHz sample rate, 8192 samples were contained in each time block corresponding to a C/A code word (1 ms). Thus, the 50,000-sample data files enabled six consecutive impulse response functions to be developed for each visible satellite. To improve the S/N ratios of the impulse responses, the six consecutive impulse responses for each satellite were combined as follows. First, the impulse responses were shifted in time delay (by no more than  $\pm 1$  time sample) to align the peaks of the power delay profiles in relative time delay. Then the impulse responses were multiplied by phase factors defined so that each of the resulting impulse responses had zero degrees of phase at the peak of the power delay profile to align the phases of the impulse responses. The impulse responses were then added coherently.

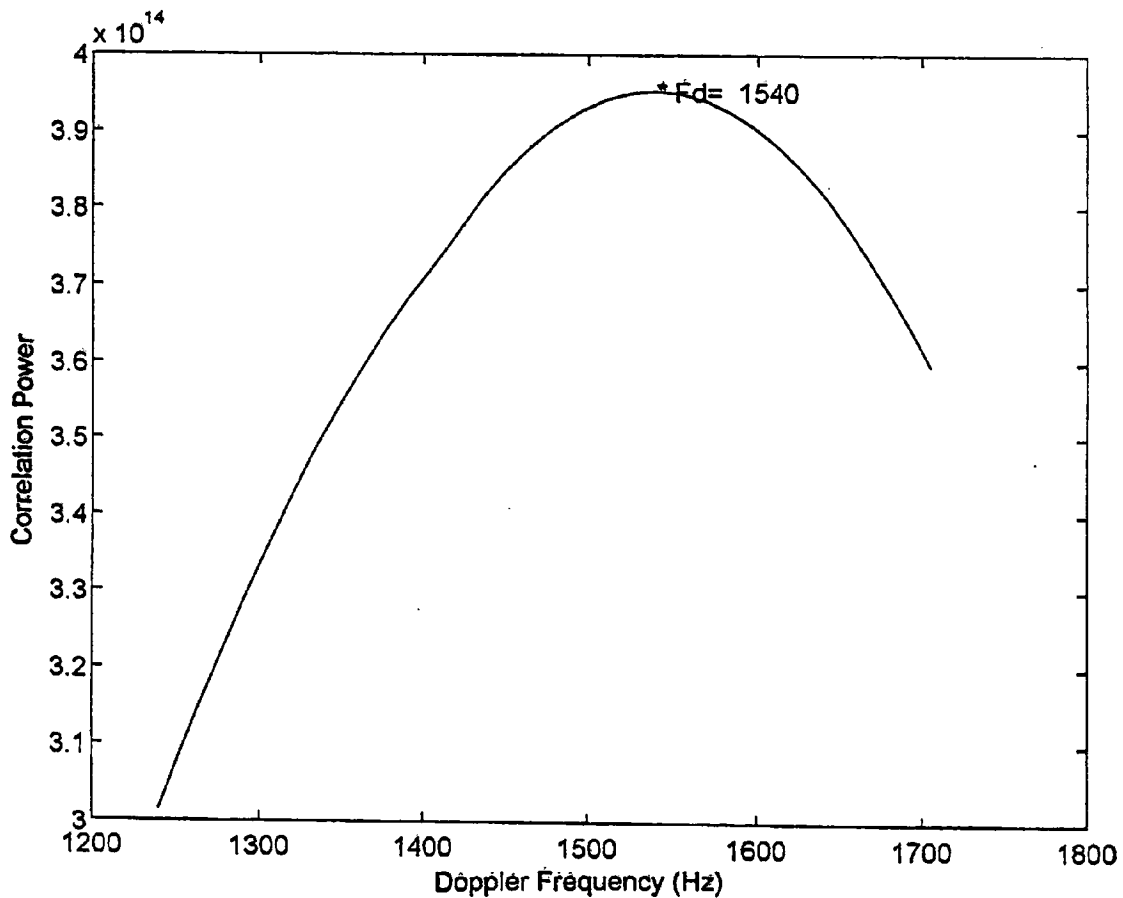
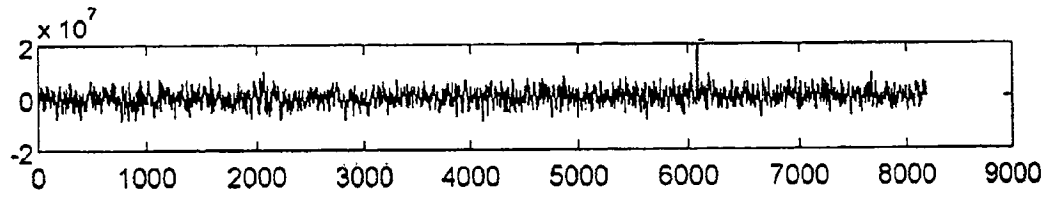


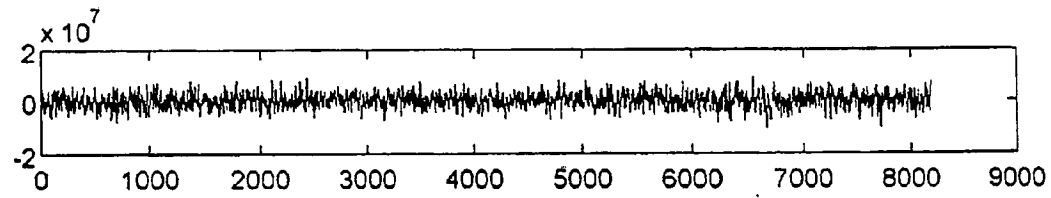
Figure 3. Correlation peak power (in arbitrary units) versus Doppler shift.

Typical results are shown in Figures 3, 4, and 5, using an IF of 1.5 MHz and the code for the BIIA-18 satellite. Figure 3 is a plot of the peak of the power delay profile (corresponding to the first code word in the data file) versus Doppler shift in Hz. A sequence of six consecutive impulse responses was developed, using the value of Doppler shift for which the correlation peak is a maximum.

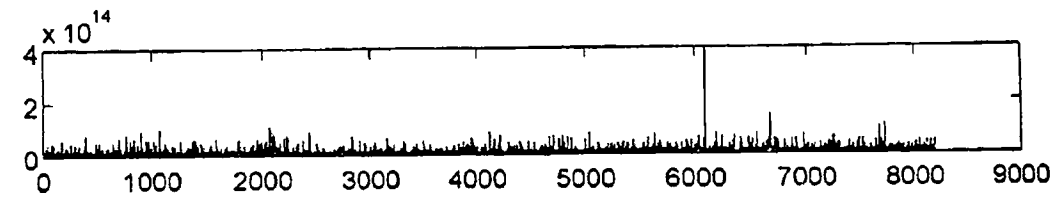
The inphase (I) and quadrature (Q) components of the impulse response corresponding to the first code word are plotted in Figure 4(a) and 4(b), respectively. The units on the vertical scales are arbitrary, because the received signal level of the data acquisition system was not calibrated (although this could be done). The units on the horizontal scales are sample number; for a sample rate of 8.192 MHz the sample time is  $0.122 \mu\text{s}$  and the entire horizontal scale (8192 samples) corresponds to 1 ms of relative time delay.



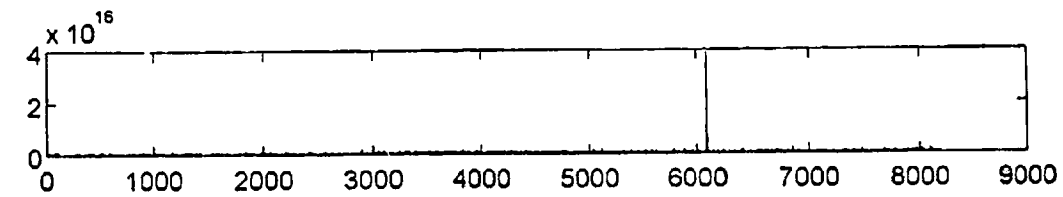
(a)



(b)



(c)



(d)

Figure 4. Plots of the (a) inphase and (b) quadrature components of an impulse response function, (c) the corresponding power delay profile, and (d) the power delay profile of the sum of six consecutive impulse responses (in arbitrary units).

The power delay profile ( $I^2+Q^2$ ) corresponding to Figures 4(a) and 4(b) is plotted in Figure 4(c). Figure 4(d) shows the power delay profile obtained by coherently combining the six consecutive impulse responses. A plot of this latter power delay profile (in dB units of relative power) is shown on magnified scales in Figure 5. The improvement in S/N ratio achieved by combining the impulse responses is clearly evident.

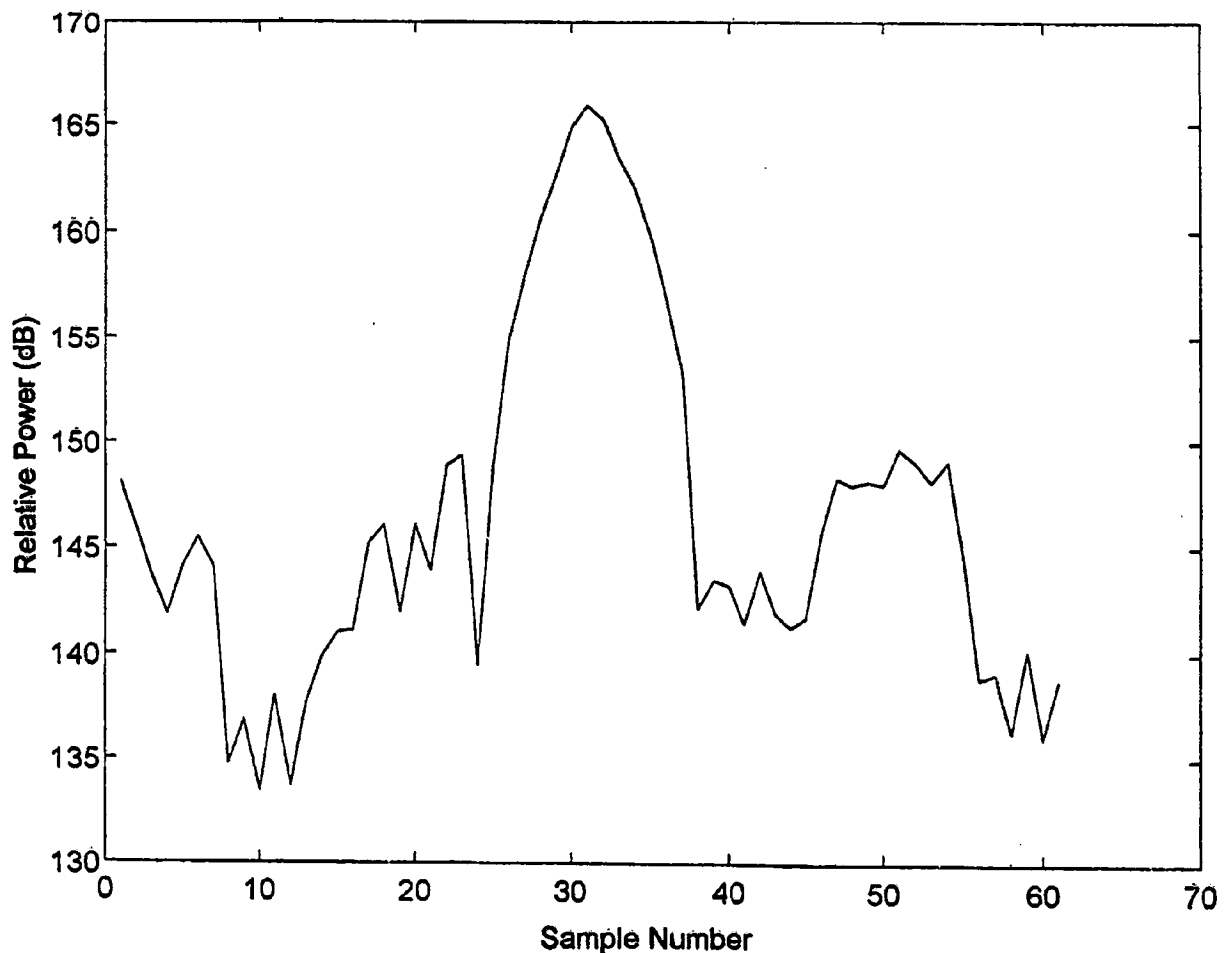


Figure 5. Plot of the impulse response function in Figure 4(d) on magnified scales.

None of the impulse responses developed from the data files shows any indication of multipath. This is not surprising, given the location of the receive antenna on a rooftop where multipath reflections from nearby terrain and buildings are unlikely to be visible. However, the results do indicate that this technique yields S/N ratios that are sufficient to reveal multipath signals that are as much as 20 dB below the power of the direct arrival.

The S/N ratios of all the impulse responses developed from the data files are summarized in Table 2. Although noise power generally refers to an average power ( $N_A$ ), it is also of interest to know the peak noise power ( $N_P$ ) in each impulse response in order to estimate the power level below which multipath signals cannot be distinguished from spurious noise peaks. Therefore, the ratios of the signal power to both the average noise power ( $S/N_A$ ) and the peak noise power ( $S/N_P$ ) were computed using the following technique.

The measured value of the impulse response at the correlation peak is the sum of the desired signal and the noise. Thus, if the noise is treated as a zero-mean random process that is uncorrelated with the signal,

$$\langle I^2 + Q^2 \rangle_0 = S + N_A, \quad (3)$$

where  $\langle I^2 + Q^2 \rangle_0$  denotes the expected value of the power delay profile at the correlation peak, and  $S$  and  $N_A$  denote the expected values of the signal power and noise power, respectively. At values of time delay far away from the correlation peak, where no signal is expected, the measured value of the impulse response is pure noise. Thus,

$$\langle I^2 + Q^2 \rangle_A = N_A, \quad (4)$$

where  $\langle I^2 + Q^2 \rangle_A$  denotes the average value of the power delay profile at values of time delay far from the correlation peak. Only samples of the power delay profile more than 50 samples (approximately 5  $\mu$ s) away from the correlation peak were used to compute the average noise power. Dividing (3) by (4), the signal-to-noise ratio ( $S/N_A$ ) is

$$\frac{S}{N_A} = \frac{\langle I^2 + Q^2 \rangle_0}{\langle I^2 + Q^2 \rangle_A} - 1. \quad (5)$$

Similarly, for the peak noise power,

$$\langle I^2 + Q^2 \rangle_P = N_P, \quad (6)$$

where  $\langle I^2 + Q^2 \rangle_P$  denotes the peak value of the power delay profile more than 50 samples away from the correlation peak and  $N_P$  is the peak noise power. Dividing (3) by (6) gives

$$\frac{S}{N_P} = \frac{\langle I^2 + Q^2 \rangle_0}{\langle I^2 + Q^2 \rangle_P} - \frac{N_A}{N_P}, \quad (7)$$

since  $N_A < N_P$ , replacing  $N_A/N_P$  by unity in (7) results in the inequality

$$\frac{S}{N_P} > \frac{\langle I^2 + Q^2 \rangle_0}{\langle I^2 + Q^2 \rangle_P} - 1, \quad (8)$$

which can be used to obtain a lower bound for  $S/N_P$ .

Strictly speaking,  $\langle I^2 + Q^2 \rangle$  is an expected value and can only be obtained from an ensemble of impulse response records. However, this was precluded by the limited size of the database. Therefore, (5) and (8) were used to estimate the S/N ratios for each of the individual impulse response records, and the results were averaged for the six consecutive records corresponding to each satellite. In addition, (5) and (8) were used to estimate the S/N ratios for the impulse responses obtained by coherently combining the six consecutive records for each satellite.

Table 2 lists the average values of  $S/N_A$  and  $S/N_P$  for two IFs (1.027 MHz and 1.5 MHz) and for two Doppler resolutions (15 Hz and 250 Hz), resulting in four values for each of the average S/N ratios for each satellite. The S/N ratios for the combined records were only computed for the 1.5-MHz IF and a Doppler resolution of 15 Hz. As can be seen from the table, using different IFs and/or different Doppler resolutions has little effect on the S/N ratios. For the two different IFs, the S/N ratios can differ by as much as a dB or more, but typically by a few tenths of a dB. The effect of changing the Doppler resolution from 15 Hz to 250 Hz is even less significant, typically on the order of a tenth of a dB. The S/N ratios show a slight tendency to increase for higher elevation angles and lower Doppler shifts.

The increases in the S/N ratios as a result of coherently combining the individual impulse responses are approximately consistent with expectations. The phases of the individual impulse responses have been adjusted so that they all have zero phase at the correlation peak. One therefore expects the peak of the coherent sum of  $N$  impulse responses to scale like  $N$ , and the power to scale like  $N^2$ . On the other hand, if one assumes the noise is a Gaussian random process, the sum of  $N$  independent, identically distributed noise processes is a Gaussian process whose variance (which equals the expected value of the power) scales like  $N$ . Therefore, one expects the S/N ratios to scale like  $N$ . For  $N = 6$ , this corresponds to an increase of 7.8 dB. The average increases in  $S/N_A$  and  $S/N_P$  for the five sets of impulse responses are 6.3 dB and 8.5 dB, respectively.

Two possible causes of concern in using the C/A codes for impulse response measurements are the autocorrelation sidelobes and the cross-correlation between codes of different satellites. However, Gold [5] has shown that relative to the central autocorrelation peak, the magnitudes of the sidelobes are bounded by the quantity

$$\frac{2^{\left(\frac{n+2}{2}\right)+1}}{P}, \quad (9)$$

where  $n$  is the number of shift register stages used to generate the codes and  $P$  is the length of the code. For the C/A codes,  $n = 10$  and  $P = 1023$ , so that the sidelobe levels are at least 24 dB down from the central peak. For Gold codes of length 1023, it can be shown [6] that the peak cross-correlation is 23.8 dB down from the autocorrelation peak. Therefore, the autocorrelation sidelobes and cross-correlation peaks of the C/A codes are not significant for the measurements discussed herein.

Table 2. Signal-to-noise Ratios of Impulse Response Measurements

Satellite	Average $S/N_A$ (dB)	Combined $S/N_A$ (dB)	Average $S/N_P$ (dB)	Combined $S/N_P$ (dB)	IF (MHz)	Doppler Resolution (Hz)	Doppler Shift (Hz)
BII-1	13.3		2.1		1.027	15	3115
BII-1	12.5	19.2	0.0	10.2	1.5	15	3155
BII-1	13.5		2.4		1.027	250	3000
BII-1	11.7		-1.6		1.5	250	3250
BII-4	11.3		-1.8		1.027	15	-2800
BII-4	12.4	18.6	0.0	9.7	1.5	15	-2770
BII-4	11.3		-2.3		1.027	250	-2750
BII-4	12.5		0.0		1.5	250	-2750
BII-6	15.0		3.9		1.027	15	-2460
BII-6	15.5	21.4	4.7	11.4	1.5	15	-2400
BII-6	14.9		3.8		1.027	250	-2500
BII-6	15.3		4.5		1.5	250	-2500
BIIA-17	15.6		4.9		1.027	15	-650
BIIA-17	15.8	22.1	4.9	11.8	1.5	15	-625
BIIA-17	15.3		4.3		1.027	250	-750
BIIA-17	15.6		4.5		1.5	250	-500
BIIA-18	14.6		2.8		1.027	15	1510
BIIA-18	14.7	21.0	3.2	12.1	1.5	15	1540
BIIA-18	14.6		2.8		1.027	250	1500
BIIA-18	14.8		3.3		1.5	250	1500

## 5. RECOMMENDATIONS FOR FUTURE WORK

The measurement results discussed above indicate that  $S/N$  ratios can be achieved that are adequate to detect multipath signals many dB below the power of the direct arrival. The absence of multipath in the data analyzed thus far can be attributed to the location of the receive antenna at a site where multipath is unlikely to be present. However, multipath may be present in some environments, and it is important for both navigation and communications applications that such multipath be measured and characterized. Aside from multipath, impulse response measurements can provide other important information about transmission channels, including received signal levels and channel

dynamics. It is therefore recommended that the following research be undertaken: incorporation of additional memory into the measurement system, additional measurements, and additional processing of the measured data.

Data files comprising 50,000 samples (at the 8.192 MHz sample rate) allow only six consecutive impulse responses to be developed. Some applications, including the computation of the channel scattering function (discussed below), require measurements of the impulse response over time histories longer than 6 ms. Additional memory could be added to the measurement system with little effort and expense. For example, 8.4 million samples would enable 1024 consecutive impulse responses to be developed.

Installation of the measurement system in a van would enable data to be collected in a variety of environments. This is important for two reasons. First, data collected in some environments (for example, urban, suburban, and mountainous terrain) may reveal the presence of significant multipath. Distributions of delay spread in various environments could be developed and the relationship between delay spread and elevation angle investigated. Second, data could be collected while the van is moving, so that the channel dynamics could be characterized. This is important for mobile radio applications as well as determining the position of moving vehicles.

The scattering function is a useful quantity for characterizing channel dynamics. It enables the display of the time-varying impulse response as a function of both time delay and Doppler shift. If one denotes time by  $t$  and time delay by  $\tau$ , the scattering function is defined as the Fourier transform (with respect to  $t$ ) of the autocorrelation function of the impulse response for each value of  $\tau$ , and is therefore the power spectrum of the impulse response for each value of  $\tau$ . As in the computation of the impulse response, it is convenient to compute the correlation integral in the frequency domain. Thus, the scattering function can be defined as the square of the Fourier transform (with respect to  $t$ ) of the impulse response:

$$S(\tau, \omega_D) = \left| \int_0^T h(t, \tau) e^{-j\omega_D t} dt \right|^2, \quad (10)$$

where  $h(t, \tau)$  is the impulse response and  $T$  is the length of time over which measurements of the impulse response are performed. The Doppler frequency ( $\omega_D$ ), not to be confused with the Doppler shift ( $\omega_{DS}$ ) due to the motion of the satellite, is the frequency variable in the power spectrum of the impulse response.

In a mobile channel, the direct signal and the multipath signals are generally associated with different Doppler shifts, because the different signal components arrive at the receiver via different propagation paths. At the L-band frequency of the GPS signals, vehicular motion can generate Doppler spreads as large as several hundred Hz in worst case scenarios. For such channels, the scattering function should be developed over a Doppler bandwidth on the order of a kHz. If the integral in (10) is evaluated as a discrete Fourier transform, the Doppler bandwidth is  $1/T$  and the



Doppler frequency resolution is the rate at which the impulse responses are measured in time. Thus, the measurement of 1024 consecutive impulse responses at the rate of one impulse response per ms would enable the scattering function to be developed over a Doppler bandwidth of 1 kHz with a resolution of approximately 1 Hz. Doppler power profiles and distributions of Doppler spread, like the corresponding quantities in the time domain (power delay profiles and distributions of delay spread), are channel characteristics that are important to system designers.

Aside from characterizing multipath and channel dynamics, impulse response measurements using GPS signals, coupled with knowledge of the elevation angles of the satellites, can provide useful information about received signal levels (RSLs) and satellite availability. The RSL for a particular satellite is proportional to the magnitude of the correlation peak in the impulse response. Such measurements could therefore provide information about the relationship between RSL and elevation angle, and could be used to develop distributions of fading rates and fade durations.

The availability of a particular satellite is determined by the presence or absence of a correlation peak corresponding to that satellite. Using impulse response measurements, the relationship between availability and elevation angle in various environments can be investigated. This is especially important for satellite communication systems that use low earth orbit satellites (LEOS), because the satellites that are available to a particular user change on a relatively short-term basis.

## 6. CONCLUSIONS

The results presented in this report clearly establish the feasibility of performing impulse response measurements over space-earth paths using the GPS C/A codes. The 1.023-MHz chipping rate of the C/A codes provides a time-delay resolution that is probably not adequate to resolve all the multipath that may be present in some channels (path differences much less than 300 m). However, this measurement resolution should be adequate to characterize the channel for applications that use a bandwidth on the order of or less than that of the measurements (2 MHz). Furthermore, the results show that the S/N ratios that can be attained are adequate to detect multipath components that are 20 dB or more below the power of the direct arrival.

An advantage of using GPS satellites to perform these measurements is that the impulse responses from several satellites whose positions are continually varying can be measured simultaneously. Thus, distributions of channel characteristics (including delay and Doppler spreads, RSLs, and satellite availability) as well as the relationships between these characteristics and satellite position (azimuth and elevation angle) can be investigated in a variety of environments. The development of such a database would provide a valuable resource for system designers in both the communications and navigation communities.

## 7. ACKNOWLEDGMENTS

The authors wish to thank Mr. John Kiebler of NASA Headquarters for funding that partially supported the work reported herein, and Dr. Faramaz Davarian for several helpful suggestions.

## 8. REFERENCES

- [1] J.J. Lemmon and R.W. Hubbard, "Multipath measurements for the land mobile satellite radio channel," MSAT-X Report No. 126, Jet Propulsion Laboratory, California Institute of Technology, Pasadena, CA, Oct. 1985.
- [2] J.J. Lemmon, "Multipath measurements for land mobile satellite service using Global Positioning System Signals," Proceedings of the Mobile Satellite Conference, Pasadena, CA, May 1988.
- [3] P.F. MacDoran, R.B. Miller, D. Jenkins, J. Lemmon, K. Gold, W. Schreiner, and G. Snyder, "Codeless GPS applications to multipath: CGAMP," Proceedings of the Fourteenth NASA Propagation Experimenters Meeting (NAPEX XIV) and the Advanced Communications Technology Satellite (ACTS) Propagation Studies Miniworkshop, Austin, TX, May 1990.
- [4] Department of Defense/Department of Transportation, "Global Positioning System Standard Positioning Service Signal Specification," Nov. 1993.
- [5] R. Gold, "Optimal binary sequences for spread spectrum multiplexing," *IEEE Trans. Info. Theory*, pp. 619-621, 1967.
- [6] J.J. Spilker, "GPS signal structure and performance characteristics," *J. Inst. Navigation*, Vol. 25, No. 2, pp. 121-146, 1978.

FORM NTIA-29 (4-80)		U.S. DEPARTMENT OF COMMERCE NAT'L. TELECOMMUNICATIONS AND INFORMATION ADMINISTRATION	
BIBLIOGRAPHIC DATA SHEET			
		1. PUBLICATION NO. 95-324	2. Gov't Accession No.
		3. Recipient's Accession No.	
4. TITLE AND SUBTITLE Impulse Response Measurements over Space-Earth Paths Using the GPS Coarse/Acquisition Codes		5. Publication Date September 1995	
		6. Performing Organization Code ITS.S3	
7. AUTHOR(S) LEMMON, JOHN J. PAPAZIAN, PETER D.		9. Project/Task/Work Unit No.	
8. PERFORMING ORGANIZATION NAME AND ADDRESS Department of Commerce/NTIA/ITS.S3 325 Broadway Boulder, CO 80303-3328		10. Contract/Grant No.	
11. Sponsoring Organization Name and Address		12. Type of Report and Period Covered NTIA REPORT	
		13.	
14. SUPPLEMENTARY NOTES			
15. ABSTRACT (A 200-word or less factual summary of most significant information. If document includes a significant bibliography or literature survey, mention it here.)  The impulse responses of radio transmission channels over space-earth paths were measured using the coarse/acquisition code signals from the Global Positioning System of satellites. The data acquisition system and signal processing techniques used to develop the impulse responses are described. Examples of impulse response measurements are presented. The results indicate that this measurement approach enables detection of multipath signals that are 20 dB or more below the power of the direct arrival. Channel characteristics that could be investigated with additional measurements and analyses are discussed.			
16. Key Words (Alphabetical order, separated by semicolons)  impulse response function; Global Positioning System (GPS), radio transmission channel; pseudorandom noise (PN) codes			
17. AVAILABILITY STATEMENT  <input checked="" type="checkbox"/> UNLIMITED  <input type="checkbox"/> FOR OFFICIAL DISTRIBUTION		18. Security Class. (This report)  Unclassified	20. Number of pages  22
		19. Security Class (This page)  Unclassified	21. Price



## **NTIA FORMAL PUBLICATION SERIES**

### **NTIA CONTRACTOR REPORT**

Information generated under an NTIA contract or grant and considered an important contribution to existing knowledge.

### **NTIA HANDBOOK**

Information pertaining to technical procedures, reference and data guides, and formal user's manuals that are expected to be pertinent for a long time.

### **NTIA MONOGRAPH**

A scholarly, professionally oriented publication dealing with state-of-the-art research or an authoritative treatment of a broad area. A monograph is expected to have a long lifespan.

### **NTIA REPORT**

Important contributions to existing knowledge but of less breadth than a monograph, such as results of completed projects and major activities, specific major accomplishments, or NTIA-coordinated activities.

### **NTIA RESTRICTED REPORT**

Contributions that fit the NTIA Report classification but that are limited in distribution because of national security classification or Departmental constraints. This material receives full review and quality control equivalent to the open-literature report series.

### **NTIA SPECIAL PUBLICATION**

Information derived from or of value to NTIA activities such as conference proceedings, bibliographies, selected speeches, course and instructional materials, and directories.

### **SPONSOR-ISSUED REPORTS**

NTIA authors occasionally produce reports issued under an other-agency sponsor's cover. These reports generally embody the criteria of the NTIA Report series.

For information about NTIA publications, contact the ITS Technical Publications Office at 325 Broadway, Boulder, CO, 80303 Tel. (303) 497-3572 or e-mail [shaw@its.blrdoc.gov](mailto:shaw@its.blrdoc.gov).

---

*This report is for sale by the National Technical Information Service, 5285 Port Royal Road, Springfield, VA 22161, Tel. (703) 487-4650.*



**NTIS does not permit return of items for credit or refund. A replacement will be provided if an error is made in filling your order, if the item was received in damaged condition, or if the item is defective.**

## ***Reproduced by NTIS***

National Technical Information Service  
Springfield, VA 22161

*This report was printed specifically for your order  
from nearly 3 million titles available in our collection.*

For economy and efficiency, NTIS does not maintain stock of its vast collection of technical reports. Rather, most documents are printed for each order. Documents that are not in electronic format are reproduced from master archival copies and are the best possible reproductions available. If you have any questions concerning this document or any order you have placed with NTIS, please call our Customer Service Department at (703) 487-4660.

### **About NTIS**

NTIS collects scientific, technical, engineering, and business related information — then organizes, maintains, and disseminates that information in a variety of formats — from microfiche to online services. The NTIS collection of nearly 3 million titles includes reports describing research conducted or sponsored by federal agencies and their contractors; statistical and business information; U.S. military publications; audiovisual products; computer software and electronic databases developed by federal agencies; training tools; and technical reports prepared by research organizations worldwide. Approximately 100,000 new titles are added and indexed into the NTIS collection annually.

For more information about NTIS products and services, call NTIS at (703) 487-4650 and request the free *NTIS Catalog of Products and Services*, PR-827LPG, or visit the NTIS Web site <http://www.ntis.gov>.

### **NTIS**

***Your indispensable resource for government-sponsored  
information—U.S. and worldwide***